A Data-Driven Fixed-Structure Control Design Method with Application to a 2-DOF Gyroscope

Christoph Kammer and Alireza Karimi

***Abstract*— This paper presents the practical aspects and application of a novel data-driven, fixed-structure, robust control design method. Only the frequency response data of the system is needed for the design, and no parametric model is required. The method can be used to design fully parametrized continuous- or discrete-time matrix transfer function controllers. The control performance is specified as constraints on the H_∞ or H_2 norm of weighted sensitivity functions, and a convex formulation of the robust design problem is proposed. An application of the presented method is explored on an experimental setup, where a multivariable controller for a gyroscope is designed based only on the measured frequency response of the system.**

I. Introduction

While model-based robust control design techniques have developed into powerful tools, practitioners often shy away from their use. Identifying a good parametric model can be difficult, and is often deemed too time-consuming and expensive in an industrial environment. On the other hand, it is generally straightforward to obtain the frequency response of a system, which is a popular and intuitive tool among practitioners. This fact, combined with the ubiquity of sensors in modern devices, makes data-driven control design methods a very attractive alternative in industrial applications [1], [2].

In recent times, several methods have been developed in the literature that combine data-driven methods with optimization-based robust control design by taking a frequency-domain approach. This makes it possible to achieve significantly better performance than previous data-driven methods.

Several convex approaches to design linearly parametrized (LP) controllers for SISO systems with a desired gain and phase margin have been proposed [3], [4]. A method to design LP controllers with loop shaping or H_∞ performance has been developed in [5], [6], [7], and is extended to MIMO systems in [8] with the use of Gershgorin bands.

Another approach for the robust design of LP-MIMO state-space controllers is presented in [9]. A method to design MIMO-PID controllers based on a linear approximation of convex-concave constraints was developed in [10], [11], although no proof of stability is given. The method is further extended in [12] and applied in [13]. In [14] a non-smooth method is used to directly solve the convex-concave optimization problem to compute fixed-structure controllers with a wide range of performance specifications. However, a common limitation of the discussed approaches is that the performance can only be specified in the H_∞ and not in the H_2 sense.

The focus of this paper is on a novel data-driven method developed in [15]. The method can be used to design fixed-structure, robust controllers based on the frequency response of multivariable systems and convex optimization. This paper aims to discuss some practical aspects of this method, and presents two comprehensive examples that demonstrate its applicability. The method allows the design of fully parametrized, multivariable transfer-function controllers either in continuous- or directly in discrete-time, which allows to skip the controller discretization step. Unlike the methods discussed above, the control performance can be specified as constraints both on the H_2 and H_∞ norm of any weighted sensitivity function. This allows for an intuitive and powerful problem formulation that is well suited for a large range of real-world control problems. It is also shown how the controller synthesis can be formulated as a convex optimization problem with linear matrix inequality (LMI) constraints.

The method has been applied in [16] to design monovariable data-driven controllers for an atomic force microscope, and in [17] to synthesize a controller for a power converter at CERN. In this paper, a more general perspective with a focus on multivariable systems is considered.

The paper is structured as follows. In Section II a theoretical exposition of the control design method is given. Section III treats the design of a multivariable discrete-time controller for a Gyroscope based only on the measured frequency response, and validates the achieved performance on an experimental setup. The paper end with some concluding remarks.

II. Control Design Method

This section will present an overview of the control design method and discuss the formulation and implementation of various typical performance specifications. For reasons of space only an abbreviated version of the method will be presented. A full theoretical exposition can be found in [15].

A. Frequency Response Data

The system to be controlled is a Linear Time-Invariant multivariable (LTI-MIMO) system represented by its frequency response $G(j\omega) \in \mathbb{C}^{n\times m}$, where m is the number of inputs and n is the number of outputs. For the rest of the paper it is assumed that the Shannon theorem is satisfied for discrete-time responses such that $G(e^{j\omega}) = G(j\omega)$, and for

C. Kammer and A. Karimi are with the Laboratoire d' Automatique, École Polytechnique Fédérale de Lausanne, 1015 Lausanne, Switzerland. Corresponding author: alireza.karimi@epfl.ch

ease of notation only $G(j\omega)$ is used. Further, define $\omega \in \Omega$, with

$$\Omega = \left\{ \omega \,\middle|\, -\frac{\pi}{T_s} \leq \omega \leq \frac{\pi}{T_s} \right\} \tag{1}$$

where T_s is the controller sampling time.

The control design method is data-driven in the sense that $G(j\omega)$ can be measured directly (e.g. sweep), or easily obtained from time-domain measurement data (e.g. Fourier analysis). Unlike with classical robust design methods, no parametric model is required, and no system identification step is necessary. Another advantage of using frequency response data as opposed to a state-space model is that time delays are represented exactly.

B. Controller Structure

The controller is defined as a fixed-structure matrix transfer function and can be formulated either in continuous- or discrete-time. As they are analogous, for reasons of space only the discrete-time definition is given. The controller is defined as $K = X(z)Y(z)^{-1}$, with:

$$\begin{aligned} X(z) &= (X_p z^p + \ldots + X_1 z^1 + X_0) \circ F_x \\ Y(z) &= (I z^p + \ldots + Y_1 z^1 + Y_0) \circ F_y \end{aligned} \tag{2}$$

where $X_i \in \mathbb{R}^{m \times n}$ and $Y_i \in \mathbb{R}^{n \times n}$ are numerical matrices containing the controller parameters. The transfer function matrices F_x, F_y contain desired fixed-terms that should be contained in the final controller, such as integrators or noise models, and $\circ$ denotes the element-wise matrix multiplication.

This form is able to accommodate a wide range of controllers (e.g. MIMO-PID, centralized, decentralized and distributed), and thanks to the full parametrization the order and structure can be chosen freely as part of the design specifications.

C. Control Specifications

Control specifications can be expressed as constraints on the norms of weighted sensitivity functions. It is interesting to note that there is no limitation on the formulation of the weighting filters $W(j\omega)$, which can be defined e.g. as transfer functions, scalar values, or arbitrary non-smooth functions such as piece-wise continuous functions. We recall some typical specifications in this section.

Performance: A classical performance criterion is to minimize the tracking error of a desired reference signal (e.g. step, ramp) in the time-domain, which is equivalent to minimizing the following H_2 norm:

$$\min_{X,Y} \|W_1 S\|_2 \tag{3}$$

where $S = (I + GK)^{-1}$ is the sensitivity function and W_1 is the Laplace transform of the reference signal.

Another typical performance specification is to minimize the H_∞ norm of weighted sensitivity functions:

$$\min_{X,Y} \|WH\|_\infty \tag{4}$$

where H can be any closed-loop sensitivity function and W is the performance weight.

The method also accommodates loop shaping, where the objective is to design a controller such that the open-loop transfer function $L = GK$ is close to a desired open-loop transfer function L_d:

$$\min_{X,Y} \|L - L_d\|_2 \tag{5}$$

The presented objective functions also lead to a decoupling of the closed-loop system if the performance criteria are chosen properly.

Robustness: Robust stability for multiplicative uncertainty

$$\mathcal{G} = G(I + W_2\Delta), \|\Delta\|_\infty < 1$$

and additive uncertainty

$$\mathcal{G} = G + W_3\Delta, \|\Delta\|_\infty < 1$$

can be guaranteed by constraining the weighted closed-loop sensitivity $T = GK(I + GK)$ and the input sensitivity $U = K(I + GK)$, respectively :

$$\|W_2 T\|_\infty < 1 \quad ; \quad \|W_3 U\|_\infty < 1$$

Finally, if a system with different frequency responses in different operating points is considered, this can be represented by a multimodel uncertainty set. This allows to design a robust controller that guarantees the performance for all operating points. Define the multimodel set as:

$$\mathcal{G}(j\omega) = \{G_1(j\omega), G_2(j\omega), \ldots, G_g(j\omega)\} \tag{6}$$

This can easily be included in the presented framework by formulating the desired performance specifications for each different model.

D. Convex Formulation of Robust Control Design Problem

The standard robust control design problems formulated in the previous section can be cast as a convex optimization problem with linear matrix inequality (LMI) constraints, which can be solved efficiently using standard solvers. The theoretical formulation leads to an infinite number of constraints (one for every frequency). A practical way to solve this issue is to define a frequency grid $\Omega_N = \{\omega_1, \ldots, \omega_N\}$ with:

$$\omega_1 \geq 0, \quad \omega_N = \frac{\pi}{T_s} \tag{7}$$

where T_s is the sampling time of the controller. Then, a set of constraint is formulated for each frequency point. The number of points should be high enough to properly represent the dynamics of the plant. Special care should be taken to include the resonance frequencies of the plant, to ensure the constraints are not violated at these points.

Furthermore, an initial controller $K_c = X_c Y_c^{-1}$ is required for the design that satisfies the following conditions:

1) The initial controller K_c and the final controller K must share the same poles on the stability boundary (the imaginary axis for continuous-time or the unit circle for discrete-time controllers).

2) The order of $\det(Y)$ must be equal to the order of $\det(Y_c)$.

It should be noted that condition 2 is not restrictive in practice. Any initial controller of lower order than the final controller can be augmented without changing its dynamics by adding an appropriate number of stable zeros and poles in X_c and Y_c such that they cancel each other.

The following paragraphs show a convex formulation of the example performance constraints in Section II-C. A thorough description on how to derive the convex formulation for other sensitivity constraints is given in [15].

Performance: Assuming a suitable frequency grid and initial controller, the performance specification $\min \|W_t S\|_2$ in (3) can be formulated as:

$$\min_{X,Y} \sum_{k=1}^{N} \text{trace}(\Gamma_k) \tag{8}$$

subject to:

$$\begin{bmatrix} \Gamma_k & W_t Y \\ (W_t Y)^* & P^* P_c + P_c^* P - P_c^* P_c \end{bmatrix} (j\omega_k) > 0$$
$$Y^* Y_c + Y_c^* Y - Y_c^* Y_c > 0$$

for all $\omega_k \in \Omega_N$, where $(\cdot)^*$ denotes the conjugate transpose and $\Gamma_k \in \{\Gamma_1, \ldots, \Gamma_N\}$ is an auxiliary matrix variable, with $P = Y + GX$ and $P_c = Y_c + GX_c$. The second constraint is necessary to guarantee the stability of the closed-loop system. It is also important to note that if the frequency points in Ω_N are not linearly spaced, a weighted 2-norm will be minimized.

For the infinity-norm in (4), as an example the convex LMI formulation of $\min \|W_1 S\|_\infty$ is:

$$\min_{X,Y} \gamma \tag{9}$$

subject to:

$$\begin{bmatrix} P^* P_c + P_c^* P - P_c^* P_c & (W_1 Y)^* \\ W_1 Y & \gamma I \end{bmatrix} (j\omega_k) > 0$$
$$Y^* Y_c + Y_c^* Y - Y_c^* Y_c > 0 \ , \ \forall \omega_k \in \Omega_N$$

where $\gamma \in \mathbb{R}$ is an auxiliary variable.

The loop-shaping problem $\min \|L - L_d\|_2$ from (5) can be formulated as:

$$\min_{X,Y} \sum_{k=1}^{N} \text{trace}(\Gamma_k) \tag{10}$$

subject to:

$$\begin{bmatrix} Y^* Y_c + Y_c^* Y - Y_c^* Y_c & (GX - L_d Y)^* \\ GX - L_d Y & \Gamma_k \end{bmatrix} (j\omega_k) > 0$$
$$\forall \omega_k \in \Omega_N$$

Robustness: The constraints $\|W_2 T\|_\infty < 1$ and $\|W_3 U\|_\infty < 1$ can be formulated as:

$$\begin{bmatrix} P^* P_c + P_c^* P - P_c^* P_c & (W_2 G X)^* \\ W_2 G X & I \end{bmatrix} (j\omega_k) > 0 \tag{11}$$
$$\begin{bmatrix} P^* P_c + P_c^* P - P_c^* P_c & (W_3 X)^* \\ W_3 X & I \end{bmatrix} (j\omega_k) > 0$$

Fig. 2. The gyroscope experimental setup by Quanser.

for all $\omega_k \in \Omega_N$.

The multimodel uncertainty from (6) can be included by formulating a set of constraints for each model. Let $P_i = Y + G_i X$ and $P_{c_i} = Y_c + G_i X_c$. Taking the sensitivity problem in (9) as an example, the convex formulation of this problem including the stability constraint would be:

$$\min_{X,Y} \gamma$$

subject to:

$$\begin{bmatrix} P_i^* P_{c_i} + P_{c_i}^* P_i - P_{c_i}^* P_{c_i} & (W_1 Y)^* \\ W_1 Y & \gamma I \end{bmatrix} (j\omega_k) > 0$$
$$Y^* Y_c + Y_c^* Y - Y_c^* Y_c > 0 \tag{12}$$
$$\text{for } i = 1, \ldots, g \quad ; \quad \forall \omega_k \in \Omega_k$$

E. Iterative Algorithm

Solving the optimization problem formulated in the previous section results in a suboptimal controller K around the initial controller K_c. Since the obtained performance can be quite far from the optimal value for the first solution, an iterative approach is used. The optimization problem is solved multiple times by using the obtained controller K as new initial controller K_c. It can be shown that this iterative approach converges to a local optimal solution of the initial non-convex problem. The procedure can be stopped once the change in the objective function is small enough, which generally happens within less than 10 iterations.

III. Data-driven Control of a Gyroscope

This experimental example presents the design of a data-driven, robust multivariable controller with multimodel uncertainty to control the gimbal angles of a gyroscope. The controller is then applied on the experimental setup to validate the performance.

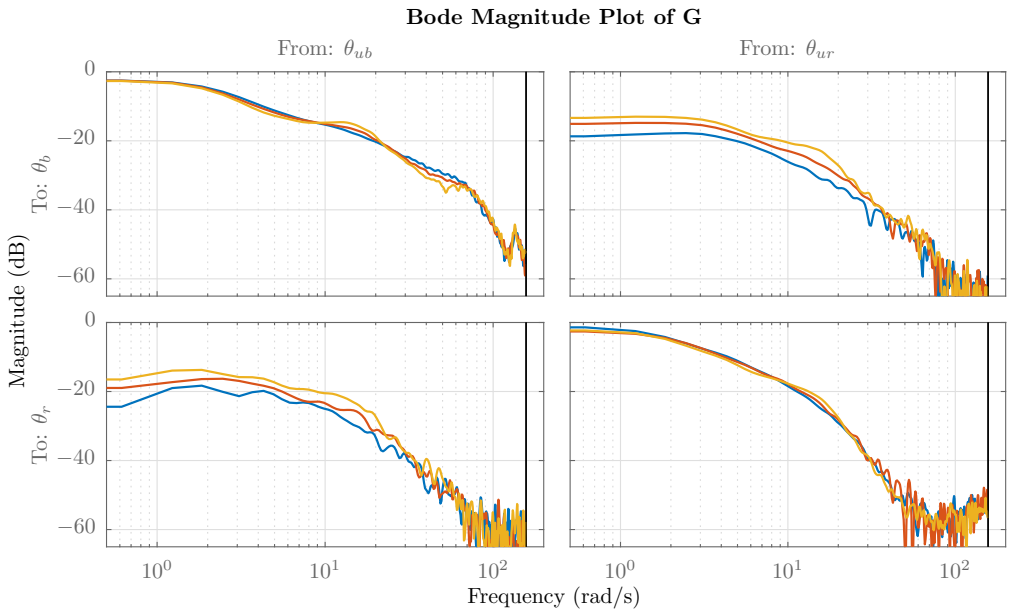

Fig. 1. The measured frequency response of the blackbox model G at different disk speeds. The blue line is the response at a disk speed of 300 rpm, red at 400 rpm and yellow at 500 rpm.

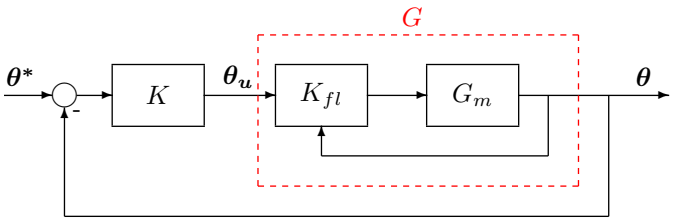

Fig. 3. Block diagram of the cascaded controller structure of the gyroscope.

A. Experimental Setup

The experiment was conducted on a 3 DOF gyroscope setup built by Quanser (see Fig. 2). The system consists of a disk mounted inside an inner blue gimbal, which is in turn mounted inside an outer red gimbal. The entire structure is supported by the rectangular silver frame. The disk, both gimbals and the frame can be actuated about their respective axis by electric motors, and their angular positions can be measured using high resolution optical encoders. For this experiment, the position of the silver frame is mechanically fixed in place. The control objective is to achieve a good tracking performance on the angular positions of the blue and red gimbal and to minimize the coupling between the axes. The dynamics of the system change depending on the angular velocity of the disk, which is included in the control design as a multimodel uncertainty.

B. Frequency Response

The gyroscope is a strongly nonlinear system, and linear control design methods only achieve good performance in a small range around the operation points. In order to improve this range, a cascaded control architecture was chosen, with a feedback linearization forming the inner loop. The block diagram in Fig. 3 shows the structure of the system, where G_m is the real plant and K_{fl} is the feedback linearization controller. The closed-loop response of the inner loop is taken as the new plant G, which is used to design the outer controller K.

The variables $\boldsymbol{\theta} = [\theta_b, \theta_r]^T$ and $\boldsymbol{\theta}^* = [\theta_b^*, \theta_r^*]^T$ are vectors containing the measured and desired blue and red gimbal angles, and $\boldsymbol{\theta_u} = [\theta_{ub}, \theta_{ur}]^T$ are the reference gimbal angles given to the feedback linearization.

The black box model G therefore has 2 inputs and 2 outputs, and a single-channel excitation is applied to calculate the frequency response of G. A PRBS signal with an amplitude of $\pm 10°$, a length of 511 samples and a sampling time of 20 ms was applied for 4 periods to θ_{ub} and θ_{ur} respectively. The non-excited input was set to zero during the process. The frequency response was calculated in Matlab using the *spa* command with a Hann window length of 150. The frequency response was measured for the three different disk velocities $\boldsymbol{v} = [300, 400, 500]$ rpm, resulting in three models $\mathcal{G} = [G_1, G_2, G_3]$. The frequency responses are shown in Fig. 1. It can be seen that the coupling and resonance modes become stronger at higher disk speeds.

C. Control Design Formulation

Based on the three frequency responses, a multivariable controller is designed. The goal is to decouple the system while also achieving good tracking performance of the reference angles θ^*. Therefore, as objective function we choose to minimize the 2-norm $\|L - L_d\|_2$ between the actual open-loop transfer function L and desired open-loop transfer function $L_d = \frac{\omega_c}{s} I$, where a bandwidth of $\omega_c = 4$ rad/s is desired for the decoupled system.

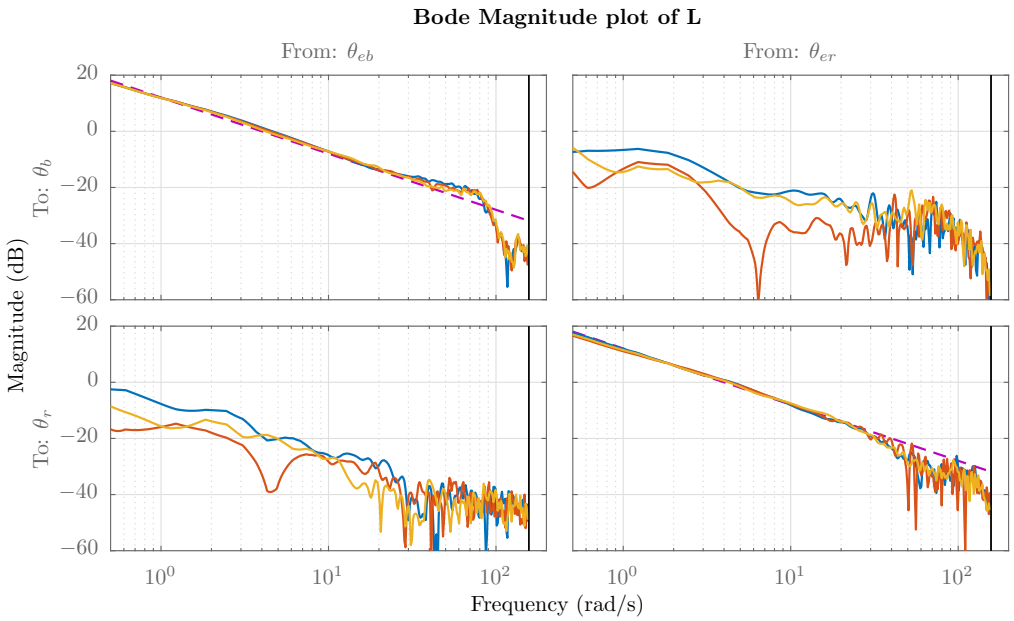

Fig. 4. Bode magnitude plots of the desired open-loop transfer function L_d and the achieved $L_{1,2,3}$ for the three different plant models. The blue line is the achieved response at a disk speed of 300 rpm, red at 400 rpm and yellow at 500 rpm. The desired L_d is shown in dashed purple.

To limit the overshoot and to guarantee the resonance mode at 10 rad/s is sufficiently damped, an additional H_∞ constraint is put on the complementary sensitivity function:

$$\|W_2 T\|_\infty < 1 \ , \ W_2(j\omega) = \frac{j\omega + 6.5}{1.05 \cdot 6.5} I \tag{13}$$

where W_2^{-1} has the form of a low-pass filter to ensure a roll-off at high frequencies. The fact that W_2 is not proper does not create any problem in practice because the constraints are evaluated only for finite values of ω. To prevent input saturation, a constraint on the input sensitivity is included:

$$\|W_3 U\|_\infty < 1 \ , \ W_3 = 0.05 I \tag{14}$$

where the magnitude of the weighting filter is chosen based on the expected worst-case disturbance.

A 5th-order discrete-time controller with a fixed integrator and a sampling time $T_s = 0.04$ s is chosen. This leads to the following structure:

$$\begin{aligned} X &= X_4 z^4 + X_3 z^3 + X_2 z^2 + X_1 z + X_0 \\ Y &= (I z^4 + Y_3 z^3 + Y_2 z^2 + Y_1 z + Y_0) \circ (z-1) I \end{aligned} \tag{15}$$

where $X_i \in \mathbb{R}^{2\times 2}$ is a full matrix and $Y_i \in \mathbb{R}^{2\times 2}$ is a diagonal matrix (i.e. the off-diagonal elements are fixed to zero). Fixing the structure of Y to be diagonal is useful in practice, as it greatly simplifies the calculation of the inverse and preserves the order of the controller. Note that the desired L_d and the weighting filters can be in continuous-time, while the designed controller is in discrete-time.

The optimization problem is sampled using $N = 500$ frequency points in the interval $\Omega_N = \left[10^{-1}, 25\pi\right]$ (the upper limit being the Nyquist frequency of the controller). The lower limit is chosen greater than zero in order to guarantee the boundedness of $L - L_d$. In fact a weighted two-norm of $L - L_d$ which is bounded is minimized.

The constraint sets are formulated for each of the three models $[G_1, G_2, G_3]$, resulting in the following optimization problem :

$$\min_{X,Y} \sum_{i=1}^{3} \sum_{k=1}^{N} \text{trace}[\Gamma_{k_i}]$$

subject to:

$$\begin{bmatrix} Y^* Y_c + Y_c^* Y - Y_c^* Y_c & (G_i X - L_d Y)^* \\ G_i X - L_d Y & \Gamma_{k_i} \end{bmatrix} (j\omega_k) > 0$$

$$\begin{bmatrix} P_i^* P_{c_i} + P_{c_i}^* P_i - P_{c_i}^* P_{c_i} & (W_2 G_i X)^* \\ W_2 G_i X & I \end{bmatrix} (j\omega_k) > 0$$

$$\begin{bmatrix} P_i^* P_{c_i} + P_{c_i}^* P_i - P_{c_i}^* P_{c_i} & (W_3 X)^* \\ W_3 X & I \end{bmatrix} (j\omega_k) > 0$$

$$k = 1, \ldots, N \quad ; \quad i = 1, 2, 3$$

As the gyroscope is a stable system, the initial controller was chosen as an integral controller with low gain. Furthermore, the condition on the order of the initial controller is satisfied by augmenting it with the right number of poles and zeros at 0: $X_c = 0.01 z^4 I$ and $Y_c = z^4(z-1)I$. It is important to note that Y_c has to contain an integrator to satisfy the first condition on the initial controller.

The optimization problem is implemented in Matlab using Yalmip [18], and solved with Mosek [19]. The iteration converges to a final controller in 10 steps. The Bode magnitude plots of L_d and the obtained $L_{1,2,3}$ for the three different plant models are shown in Fig. 4. It can be seen that the designed controller approximates the desired loop shape well at low frequencies, and that the system is well decoupled. The singular value plots of the obtained closed-loop and

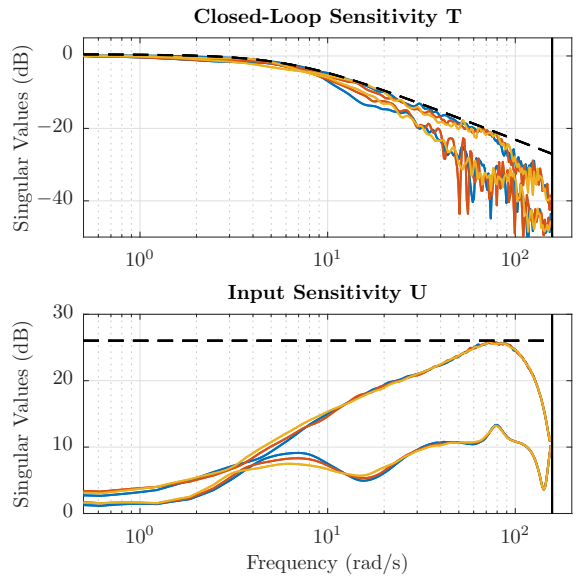

Fig. 5. Singular value plots of the achieved closed-loop and input sensitivity for the three different plants. The dashed lines indicate the constraints.

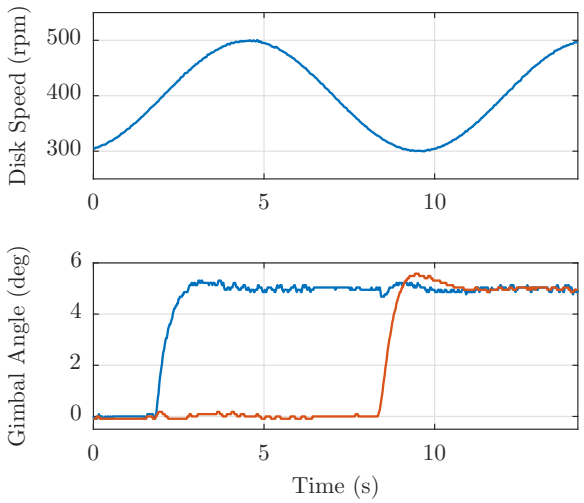

Fig. 6. Step response of the blue and red gimbal angles during a varying disk velocity.

input sensitivity are displayed in Fig. 5. It can be seen that the constraints are satisfied for all three plant models.

D. Experimental Results

To validate the results, the controller was applied on the experimental setup. The step responses of the blue and red gimbal angle were measured for varying disk speeds, and the results are shown in Fig. 6. It can be seen that the decoupling is good, and that the multimodel uncertainty introduced by the varying disk speed is handled well. The rise time is 0.625 s for the blue and 0.486 s for the red gimbal angle, which matches well the desired bandwidth specified for L_d. Furthermore, the overshoot is limited to less than 10 %.

IV. Conclusion

A data-driven method for the robust design of fixed-structure multivariable controllers was presented. The method enables the design of complicated controllers with both H_2 and H_∞ control specifications based solely on the frequency response of the system, and no modeling or system identification is required. An example demonstrated the design a low-order multivariable controller for a 2-DOF gyroscope, and the achieved performance was validated on an experimental setup.

References

[1] Z. S. Hou and J. X. Xu. On data-driven control theory: the state of the art and perspective. *Acta Automatica Sinica* 35(6), pages 560–667, 2009.

[2] Z. S. Hou and Z. Wang. From model-based control to data-driven control: Survey, classification and perspective. *Information Sciences*, 235:3–35, 2013.

[3] M. Saeki. Data-driven loop-shaping design of PID controllers for stable plants. *International Journal of Adaptive Control and Signal Processing*, 28(12):1325–1340, 2014.

[4] A. Karimi, M. Kunze, and R. Longchamp. Robust controller design by linear programming with application to a double-axis positioning system. *Control Engineering Practice*, 15(2):197–208, 2007.

[5] A. Karimi and G. Galdos. Fixed-order H_∞ controller design for non-parametric models by convex optimization. *Automatica*, 46(8):1388–1394, 2010.

[6] A. Karimi, A. Nicoletti, and Y. Zhu. Robust H_∞ controller design using frequency-domain data via convex optimization. *International Journal of Robust and Nonlinear Control*, available online `https://doi.org/10.1002/rnc.3594`, 2016.

[7] E. Thalmann, Y. J. Regamey, and A. Karimi. High performance control of a corner cube reflector by a frequency-domain data-driven robust control method. In *American Control Conference (ACC), 2016*, pages 455–460. Ieee, 2016.

[8] G. Galdos, A. Karimi, and R. Longchamp. H_∞ controller design for spectral MIMO models by convex optimization. *Journal of Process Control*, 20(10):1175–1182, 2010.

[9] M. Saeki, M. Ogawa, and N. Wada. Low-order H_∞ controller design on the frequency domain by partial optimization. *International Journal of Robust and Nonlinear Control*, 20(3):323–333, 2010.

[10] M. Hast, K. J. Astrom, B. Bernhardsson, and S. Boyd. PID design by convex-concave optimization. In *Control Conference (ECC), 2013 European*, pages 4460–4465. IEEE, 2013.

[11] S. Boyd, M. Hast, and K. J. Åström. MIMO PID tuning via iterated LMI restriction. *International Journal of Robust and Nonlinear Control*, 26(8):1718–1731, 2016.

[12] P. Mercader, K. J. Åström, A. Banos, and T. Hägglund. Robust PID design based on QFT and convex–concave optimization. *IEEE Transactions on Control Systems Technology*, 25(2):441–452, 2017.

[13] S. Shinoda, K. Yubai, D. Yashiro, and J. Hirai. Multivariable controller design evaluating closed-loop interaction by iterative LMI optimization using frequency response data. In *International Conference on Advanced Mechatronic Systems (ICAMechS)*, pages 429–434, 2015.

[14] P. Apkarian and D. Noll. Structured H_∞-control of infinite dimensional systems. *arXiv:1707.02052 [math.OC]*, 2017.

[15] A. Karimi and C. Kammer. A data-driven approach to robust control of multivariable systems by convex optimization. *Automatica*, 85, pages 227–233, 2017.

[16] C. Kammer, A. P. Nievergelt, G. Fantner, and A. Karimi. Data-driven controller design for atomic-force microscopy. In *Proceedings of the 20th IFAC World Congress*, 50(1), pages 10437–10442, 2017.

[17] A. Nicoletti, M. Martino, and A. Karimi. A data-driven approach to power converter control via convex optimization. In *Control Technology and Applications (CCTA), 2017 IEEE Conference on*, pages 1466–1471. IEEE, 2017.

[18] J. Löfberg. YALMIP: A toolbox for modeling and optimization in MATLAB. In *CACSD Conference*, `http://control.ee.ethz.ch/joloef/yalmip.php`, 2004.

[19] MOSEK ApS. *The MOSEK optimization toolbox for MATLAB manual. Version 7.1*, 2015.